Geophys. J. Int. (2001) **146,** 171–180

Point-source inversion neglecting a nearby free surface: simulation of the Underground Research Laboratory, Canada

J. Šílený[1], I. Pšenčík[1] and R. P. Young[2]

[1] *Geophysical Institute, Academy of Sciences of the Czech Republic, Boční* II/1401, 141 31 *Praha* 4, *Czech Republic. E-mail: jsi@ig.cas.cz*
[2] *Applied Seismology Laboratory, Department of Earth Sciences, Liverpool University,* 4 *Brownlow Street, Liverpool,* L69 7GP, *UK*

Accepted 2001 February 8. Received 2001 January 30; in original form 2000 February 28

SUMMARY

The aim of this study was to investigate the effects of the inconsistency between the model used and the actual structure on the inversion of point-source parameters. Specifically, we studied the effects of ignoring a reflecting interface in the model. Such a situation frequently occurs when events with sources close to mine excavations are recorded and subsequently processed using a simplified model describing the interface only approximately or ignoring it completely. In this case, it is important to ask how reliable the retrieved mechanism is. An inversion algorithm with indirect parametrization of the source (INPAR) was applied.

A numerical study was performed, in which the mechanism and source time function of a point source were sought in a model inconsistent with the actual structure. The ray synthetic wavefield generated by a source situated close to a free surface of a homogeneous half-space was treated as the observed data. The free surface was then ignored when constructing the Green's function necessary for the point-source inversion. Thus, the inconsistent response of the medium including only direct phases was used to invert the observed seismograms, which contain both direct and reflected phases. The configuration of the Underground Research Laboratory (URL) of the Atomic Energy Canada Ltd. was simulated in the synthetic experiments. 16 triaxial sensors were situated around the underground tunnel, the face of which was taken to represent the free surface near the hypocentre. High-frequency seismograms were synthetized with a frequency of around 10 kHz. This is close to the prevailing frequency of the actual URL records. It was found that gross features of the source such as orientation of the double couple and the general features of the source time function can be retrieved satisfactorily when the hypocentre is localized correctly. Formal error analysis, however, yields rather large error estimates due to the omission of the free surface, providing us with acceptably constrained solutions at about 70 per cent confidence level only. Mislocation of the hypocentre of the order of seven to 14 wavelengths and/or contamination of the data by noise with an amplitude amounting to 20 per cent of the data amplitude both distort retrieved source parameters and make them rather uncertain. The retrieved orientation deviates by more than 20° and its 70 per cent confidence region extends several tens of degrees. As a consequence of the mismodelling of the medium represented by the neglect of the free surface, spurious non-double couple (DC) components appear in the mechanism.

Two URL events from 1991 September 25 separated by 4 s were processed, and a large majority of the compensated linear-vector dipole (CLVD) was found there. The CLVD along the *P*-axis at the earlier event was replaced by the CLVD along the *T*-axis at the following one, which suggests an over-relaxation of the stress during the first event and its partial restoration by the subsequent event.

Key words: interface, inversion, seismic waves, source mechanism.

1 INTRODUCTION

When studying weak mine tremors, the fact that tremors are generated by sources situated close to mine excavations is a problem often encountered. The recorded wavefield contains not only direct waves but also reflections from the mine walls. This means that the use of a full space Green's function for retrieval of the parameters of the source situated near to a stope face is inadequate. Moreover, the direct and reflected phases can interfere and become inseparable. Radiation of energy from a source situated close to an interface is rather different from the radiation of the same source situated in a continuous medium, see, e.g. Jílek & Červený (1996) and Červený (2000).

In practice, the characteristics of the medium containing the source are usually not well known. Insufficient knowledge of these characteristics is detrimental to the processing of the high-frequency content of the signals because short wavelengths are more affected by small details of the medium, which are only rarely known well. Thus we may expect difficulties, especially in studies on a local scale, particularly when investigating mining-induced events. The location of weak mining tremors occurring near a stope face is usually not known accurately enough to allow us to determine the distance of the source from the free surface of the stope. Therefore, it is difficult to model the source exactly in the vicinity of an interface. A possible simplification is to ignore the interface and to invert the complex wavefield including both direct and reflected phases by using a simple Green's function corresponding to a direct wave only.

In this paper we study how the mechanism of the source and the source time function are affected by such inconsistent modelling. An inaccurate model of a medium may also cause the source to be inaccurately located. Therefore, as well as modelling the effect of an inconsistent medium, we also investigate the consequences of mislocation of the source. The combined effects of these inconsistencies and the effect of random noise in the data are also studied.

In local studies based on small-scale configurations, a homogeneous medium is often assumed. The reasoning behind this simplification may sometimes be sound as, for example, in the Underground Research Laboratory (URL) experiment where a tunnel has been mined out in an intact and massive plutonic rock (Young & Collins 1993). In other cases it may be a consequence of a lack of knowledge of the medium. Taking this into account, we conduct our study with a homogeneous medium because the velocity gradient attached to the free surface that was observed in the URL (Carlson & Young 1993; Falls & Young 1998) does not affect ray-paths in our set-up. The ray method is used to calculate the 'observed' wavefield generated by a dislocation point source situated close to a free surface simulating the face of the tunnel.

The algorithm of Šílený *et al.* (1992) and Šílený (1997) for the inversion of waveforms is used to retrieve the mechanism and the source time function (STF). In this INPAR algorithm (applying the INdirect PARametrization of the source) the process of source parameter retrieval is divided into two steps: (i) inversion of the waveforms into independent moment tensor rate functions (MTRFs)—time functions corresponding to individual components of the moment tensor, which essentially follows the method by Sipkin (1982), and (ii) reduction of the MTRFs into the moment tensor and the STF (Šílený 1998). This approach has been proven to work well when the inhomogeneity of the medium was simplified (Kravanja *et al.* 1999), or anisotropy of the medium was modelled incorrectly (Šílený & Vavryčuk, 2000). Thus we also anticipate it will perform well for the case of a neglected interface in the vicinity of the tremor focus.

By neglecting the interface in the model of the medium we introduce a systematic error into the forward modelling of the wavefield, which is difficult to quantify because the formal error estimates are designed for random errors, mostly with Gaussian distribution. Thus the most appropriate estimate of the error due to mismodelling of the medium is to observe the bias of the retrieved source in the synthetic experiment, which is the goal of this study. Nevertheless, we add the formal estimate of the error obtained by transforming the change of the Green's function due to neglecting the interface into the mechanism and the STF. The simplistic approach consists of generating the synthetic seismograms d_A and d_B by using Green's functions G_A and G_B, corresponding to the medium with and without the interface, respectively,

$$d_A = G_A\, m,\ d_B = G_B\, m,$$

where m is the source obtained by solving the inverse problem with 'observed' data d, $d = G_A\, m$. Then, we use the difference $|d_A - d_B|$ in the L_2 norm as a rough estimate of the standard deviation of the data, needed as the input of the formal estimate of the error of the model parameters in the inverse problem (e.g. Tarantola 1987). The procedure developed within the INPAR method in Šílený (1998) in particular was applied.

2 EXPERIMENTAL PROCEDURE

The configuration of our experiment mimics the configuration in the URL (Young & Collins 1993) (Fig. 1). We substituted the face of the tunnel with an infinite free-surface plane. The structure surrounding the tunnel was considered homogeneous, with a P-wave velocity of 6.0 km s^{-1}, an S-wave velocity of 3.5 km s^{-1} ($\sqrt{3}$ times slower than the P velocity) and a density of 2.9 g cm^{-3}. Sixteen three-component sensors were situated in front of the tunnel face with hypocentral distances ranging from 11 to 45 m (Fig. 1). The Cartesian coordinate system connected with the tunnel is used in our study. Its origin is situated at the centre of the tunnel face. The x-axis lies along the axis of the tunnel, with the positive direction pointing in the direction of excavation. The z-axis is vertical, positive up. The y-axis is chosen so that the whole system is right-handed. In this coordinate system, all sensors have a positive x-coordinate (Fig. 1). A pure shear-slip source with both strike-slip and dip-slip components situated close to the face of the tunnel is considered. A sharp source time function is used which is formed by a single peak 0.1 ms wide; its maximum frequency is about 20 kHz (Fig. 2).

For the above configuration, ray synthetic seismograms were calculated using a modified version of the software package developed by Gajewski & Pšeňík (1990) [ANRAY]. The seismograms contained converted and unconverted reflections from the free surface, in addition to the direct waves. The synthetics generated in this way were treated as 'observed' data. Due to the configuration of the stations and the frequency content of the STF, the direct and reflected waves are well separated,

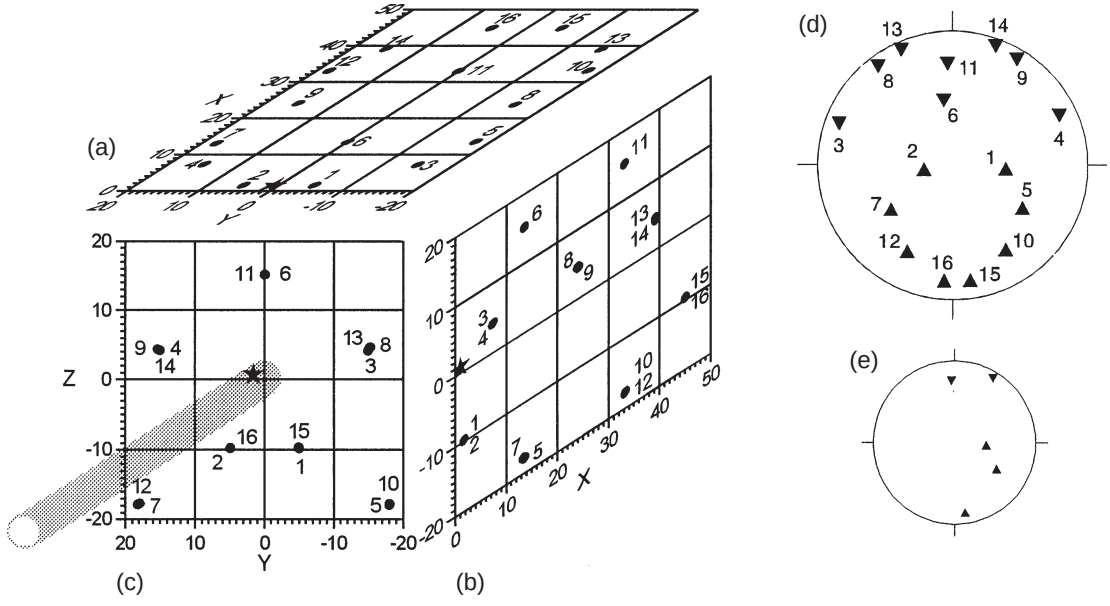

Figure 1. Station configuration in the URL, Canada. (a) plan view, (b) vertical cross-section along the x-axis and (c) vertical cross-section along the y-axis; ★ = hypocentre, ● = stations, distances in metres. Plane (y, z) represents free surface simulating the stope face, position of the tunnel marked in grey. (d) Equal-area projection of lower focal hemisphere with all 16 stations of the network, ▲ = stations below the hypocentre, ▼ = stations above the hypocentre. (e) reduced station configuration using five stations only (1, 5, 9, 11, 15).

see Fig. 3. The signal has a predominant P-wavelength of about 0.2 m, thus the source situated at a distance of 0.93 m from the free surface can be considered to be well separated from the surface.

Inversions were performed with Green's functions in which the reflected phases are ignored. The calculations are performed for three positions of the source: (i) exact location (EH) (i.e. Green's function is constructed for the same source point as the observed data), (ii) mislocation in the direction perpendicular to the free surface (MX) (Green's function constructed for the source shifted by 1.5 m away from the free surface along the x-axis), and (iii) mislocation in the direction along the free surface (MY) (Green's function constructed for the source shifted by 3 m along the positive y-axis). Looking at the configuration through the prevailing P wavelength of the used signal, we can conclude that both mislocations are significant, i.e. they are larger than the prevailing wavelength.

3 NUMERICAL EXPERIMENTS: NOISE-FREE DATA

3.1 Exact source location

Inversion gives a fairly good estimate of the source parameters, Fig. 4 (EH) the match of the synthetics to the observed data for stations 1 and 16 is given in Fig. 3. The orientation of the mechanism is systematically deviated from the true source, *cf.* Figs 2 and 4. This is the most pronounced consequence of the inconsistency in the modelling of the medium. This is confirmed by the confidence region corresponding to the nodal lines and the P and N axes, which are constructed to take the free interface missing in the Green's function into account. The dark area marking the 70 per cent confidence zone is large enough to contain both the solution obtained and the true source model. Thus, at this level, the orientation of the true source is contained in

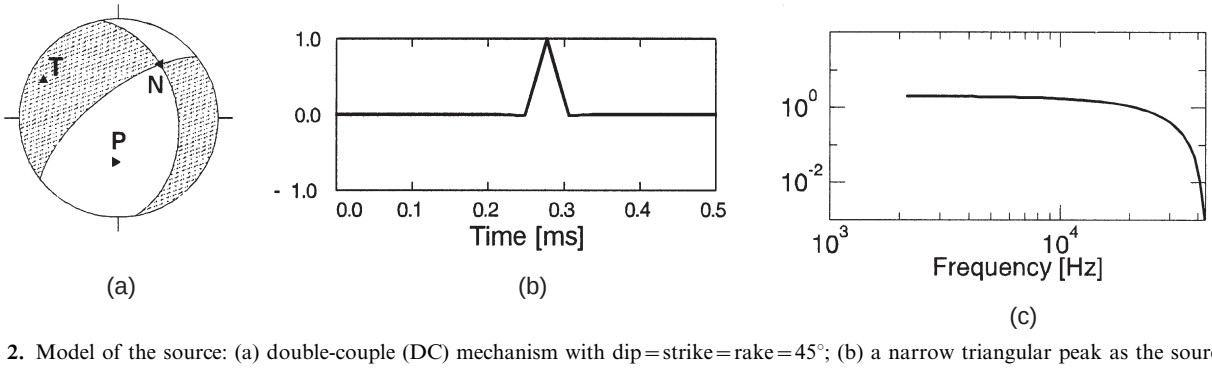

Figure 2. Model of the source: (a) double-couple (DC) mechanism with dip = strike = rake = 45°; (b) a narrow triangular peak as the source time function, (c) its spectrum.

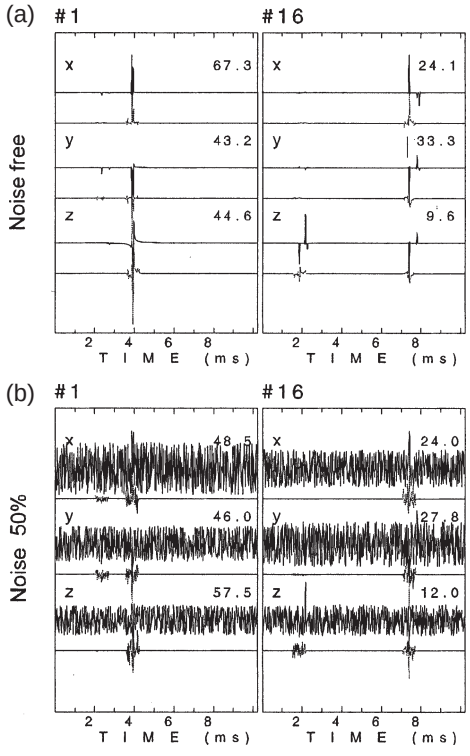

Figure 3. The observed seismograms (upper trace) for stations 1 and 16 versus synthetics (lower trace) obtained from inversion with the exact source location. (a) Noise-free seismograms, (b) seismograms contaminated by a uniform random noise reaching 50 per cent of the data peak amplitude.

our solution as well. The 80 per cent confidence zone of the *P* and *N* axes is stretched excessively in the plane perpendicular to the *T* axes (Fig. 4, EH), which indicates that there is larger uncertainty in the determination of *P* and *N* axes than in that of the *T* axis. In other words, the inexact modelling of the Green's function allows the retrieved mechanism to rotate around the *T* axis in the 80 per cent confidence level. The other effect of neglecting the free surface is the appearance of the non-double-couple component in the retrieved mechanism (Table 1). The 70 per cent confidence zone of the total moment tensor solution in the Riedesel–Jordan plot (Fig. 4, EH) crosses the locus of deviatoric solutions and touches the pure DC symbol, which means that within this confidence level the non-DC components of the retrieved moment tensor are not significant. The reconstructed STF is not far from the true one: the minor peaks accompanying the principal peak which appear as a consequence of neglected reflections are very small. From the STF confidence zone we can conclude that only the major peak is significant in the 70 per cent confidence level. The other peaks are insignificant because their confidence zone contains the zero line.

Successful recovery of the STF in this case of exact location of the hypocentre is due mainly to the application of the algorithm INPAR, which is inherently capable of reducing the artefacts of inconsistent modelling of the response of the medium (Campus *et al.* 1996; Kravanja *et al.* 1999). After deconvolving the Green's function from the seismograms, the features of the records not modelled in the Green's function appear in the independent MTRFs as non-correlated signals across the set of six functions and they are eliminated subsequently during the search for the correlated part of the MTRFs. In our case of neglecting reflections from the free surface in the response of the medium, the reflected waves appear in the MTRFs as signals additional to the peak corresponding to the direct wave. Due to the varying time delays of reflected waves behind the direct wave in individual stations, the fictitious pulses in individual MTRFs are positioned at different times and should be substantially suppressed in the search for the correlated part of the MTRFs. This is illustrated in Fig. 5, which shows MTRFs deconvolved from seismograms. The STF found as the correlated non-negative parts of the MTRFs is shown on the bottom of Fig. 5. The false signals due to the reflected waves not considered in Green's function are clearly visible. In the M_{23} moment tensor rate function, the false signals both precede and follow the actual peak at 0.2 ms. In the M_{11} trace, the false signals even

Table 1 Distortion of the mechanism and source time function retrieved in the experiments described in sections 3–5 with respect to the true source model. Deviation of the orientation of the mechanism evaluated as the average of the deviations of the principal axes. Per centage definition: p(isotropic part) + p(deviatoric part) = 100, p(DC) + p(CLVD) = 100.

Configuration	Noise	Localization	Distortion of mechanism			STF correlation	M_0/ M_0(model)
			Deviation [deg]	Isotropic [%]	CLVD [%]		
16 stations	No	EH	16	4	1	0.945	1.1
		MX	22	0	64	0.833	1.25
		MY	30	6	32	0.778	0.52
	50%	EH	8	5	2	0.894	1.58
		MX	16	3	57	0.784	1.69
		MY	25	10	38	0.592	0.84
5 stations	No	EH	15	3	33	0.934	1.43
		MX	29	3	6	0.931	1.31
		MY	43	25	42	0.894	1.25
	20%	EH	15	5	40	0.887	1.64
		MX	33	11	15	0.902	1.47
		MY	42	26	40	0.852	1.54

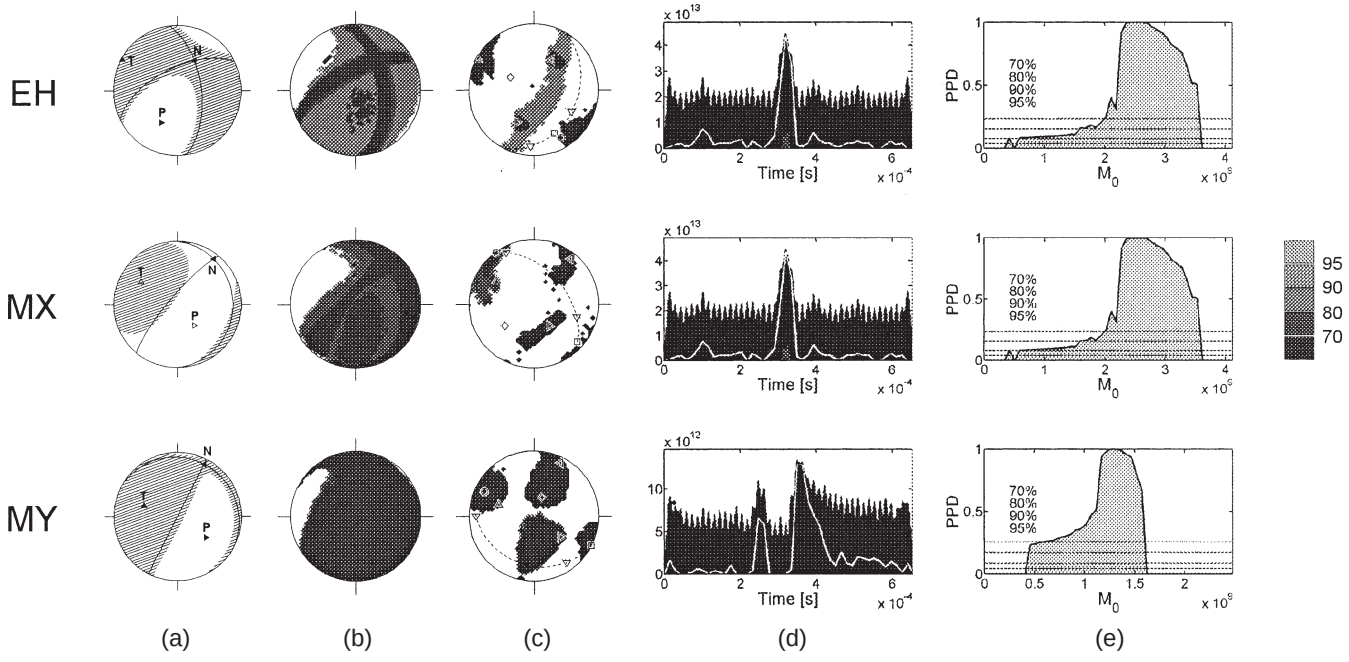

Fig. 4 Inversion of noise-free seismograms including the direct and reflected phases by using a simplified Green's function (GF) corresponding to the direct wave only. 16 stations considered. EH: GF constructed at the exact source location; MX: GF constructed at a point mislocated by 1.5 m, perpendicularly to the free surface; MY: GF constructed at a point mislocated by 3 m, parallel to the free surface. (a) Traditional fault-plane solution plot: solid lines–nodal lines of the DC part of the moment tensor (MT), shaded zones–compressions corresponding to the full MT, T–tension axis, N–null axis, P–pressure axis. (b) Confidence zones of the nodal lines of the DC part of the MT, for the confidence level see the scale of grades of shade. (c) Plot of the mechanism in the formalism by Riedesel & Jordan (1979) together with confidence zones for the full MT and the T, N and P axes. $\triangle$ = T-axis, $\triangleleft$ = N-axis, $\triangleright$ = P-axis, $\bigcirc$ = full MT, $\square$ = pure DC, $\diamond$ = pure isotropic source, $\triangledown$ = pure compensated linear-vector dipole (CLVD), dashed line = locus of deviatoric solutions. (d) retrieved source time function (white line) with its confidence zone. (e) estimate of posterior probability density (PPD) of the scalar moment M_0. Horizontal lines mark the areas containing specified probability content, their intersection with the PPD curve constrains the M_0 confidence intervals.

override the actual signal, which is weak due to the mechanism of the source. Despite the presence of the spurious signals in the MTRFs, the resulting STF predominantly contains the true source peak only. Due to the large STF confidence zone, the retrieved scalar moment M_0 is determined with large uncertainty (Fig. 4e, EH) the intersection of the posterior probability density (PPD) curve with the line marking the 70 per cent confidence level specifies a rather wide interval of acceptable values for M_0 ranging from about $2 \times 10^9 - 3.5 \times 10^9$ N m.

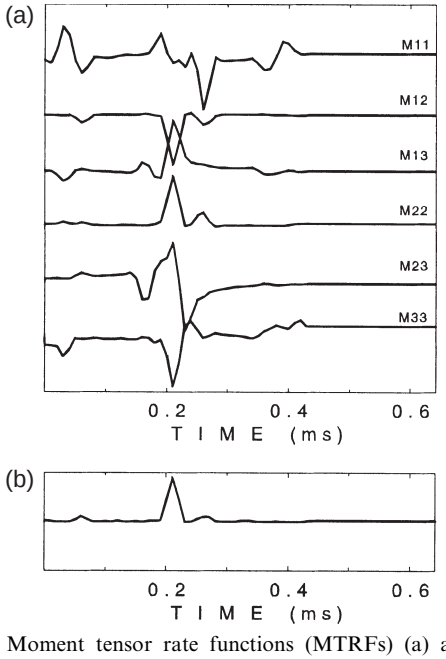

Figure. 5. Moment tensor rate functions (MTRFs) (a) and corresponding STF obtained in inversion with the exact source location (b).

In the experiment with exact source location, there was an exact fit of arrival times of synthetic and 'observed' direct waves. The reflected phases, do not exhibit the same delay from the direct phases across all the stations and thus they are efficiently ignored by the algorithm. Since, however, the exact location of the source is, as a rule, unknown, the following two experiments were designed, in which the benefit of exactly correlated arrivals of the direct phases was violated. The correlation was violated by assuming a mislocation of the hypocentre in the two directions described below.

3.2 Mislocation perpendicular to the interface

The shift amounting to 1.5 m represents more than seven prevailing P wavelengths. The 'twofold' inconsistency, where the effects of the inconsistent structure and of the incorrect source location are merged together, is expressed in the larger distortion of the reconstructed DC, in large spurious non-DC components in the source mechanism (Table 1) and in a rather high false peak in the STF Fig. 4, MX. Despite the relatively large deviation of the reconstructed DC orientation from the true source model, the 70 per cent confidence zone contains the true nodal lines, which indicates that our solution contains the true source as well. As in Section 3.1, a rotation around the T axis is allowed

but here already in the 70 per cent confidence level. In the STF, again only the major peak is significantly retrieved at the 70 per cent level.

3.3 Mislocation parallel to the interface

The result is very similar to Section 3.2, *cf.* Fig 4 MX and MY, despite the fact that this mislocation is twice as large (3 m in the direction of the y-axis). This should not be a surprise because with the parallel shift of the source, the differences in arrival times of reflected waves are smaller than with the perpendicular shift, which could effectively reduce the inconsistency in comparison with the source mislocation perpendicular to the interface. However, taking into account the error expressed by the 70 per cent confidence zone, we have to conclude that this mislocation is more harmful than Section 3.2 because the resulting mechanism and the STF become completely uncertain. Two peaks were reconstructed in the STF, but the confidence zones of both contain the zero lines which indicates that none is significant. The scalar moment is severely underestimated—its 70 per cent confidence interval ranges from 5×10^8 to about 1.6×10^9 N m, which is much less than the true value.

4 NUMERICAL EXPERIMENTS: NOISY DATA

Seismic records are always contaminated by noise, therefore it is necessary to test the sensitivity of the reconstruction of the source parameters determined from inconsistent structure models and source locations to the presence of spurious background noise in the data. Seismic noise can have very complex characteristics depending on a particular site. For simplicity, we assume a random noise with uniform distribution and a frequency content close to the spectrum of the inverted signals (Fig. 3b). We generate various amplitudes of such noise and explore up to which level the retrieval of the mechanism and the STF is still satisfactory.

In the experiment with the true source location, the orientation of the retrieved mechanism and the STF are surprisingly stable even with high levels of noise contamination (Fig. 6a). With the noise reaching 50 per cent of the peak data amplitude, inversion still yields fairly good estimates of the STF (with the significant major peak) and of the orientation of the mechanism within the systematic deviation occurring in the noise-free experiments, *cf.* Figs 4a and 6a. Similarly to the inversion of noise-free data, the experiments with both perpendicular and parallel mislocation yield solutions which are already uncertain at the 70 per cent level. It should be noted that the noise level applied here is very high in comparison with real samples still worth processing. This high level of noise was chosen to allow the robustness of the inversion with exact hypocentre to be demonstrated. With such noise contamination the hypocentre could never be located exactly in practice and a mislocation would necessarily occur.

5 NUMERICAL EXPERIMENTS: REDUCED DATA SET

The configuration of 16 stations in the URL represents an extremely ideal situation not often met in practice. Therefore, we performed experiments with noise-free and noisy data as described above, but with records of five selected stations only. This set-up models situations commonly encountered in practice more realistically. The subset of five stations is formed with stations 1, 5, 9, 11 and 15 (Fig. 1e) and the results are shown in Fig. 7.

Inversion of noise-free data at the five-station subset yields roughly the same quality of reconstruction of the orientation of principal axes as the processing of all 16 stations, the content of spurious non-DC components is larger (Table 1) and the errors

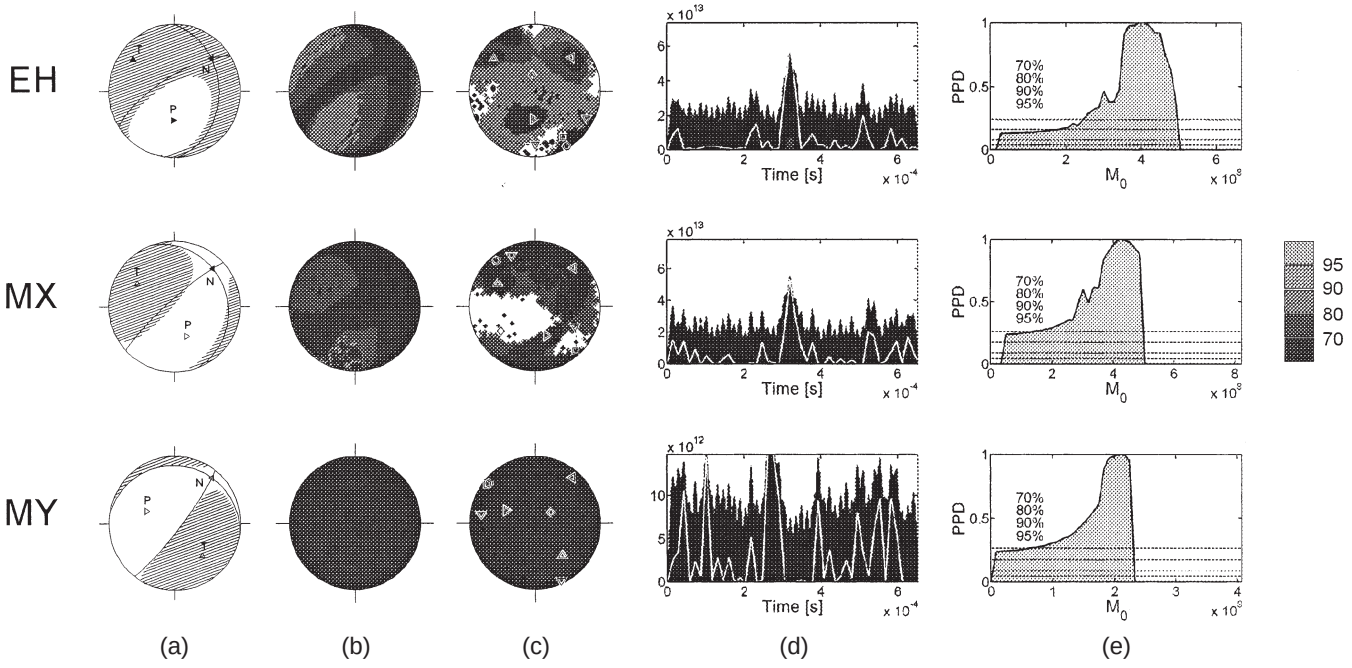

Figure 6. Inversion of noisy seismograms including the direct and reflected phases by using simplified Green's function (considering direct wave only). 16 stations considered. Uniform noise reaching 50 per cent of data peak amplitude. For details see the caption of Fig. 4.

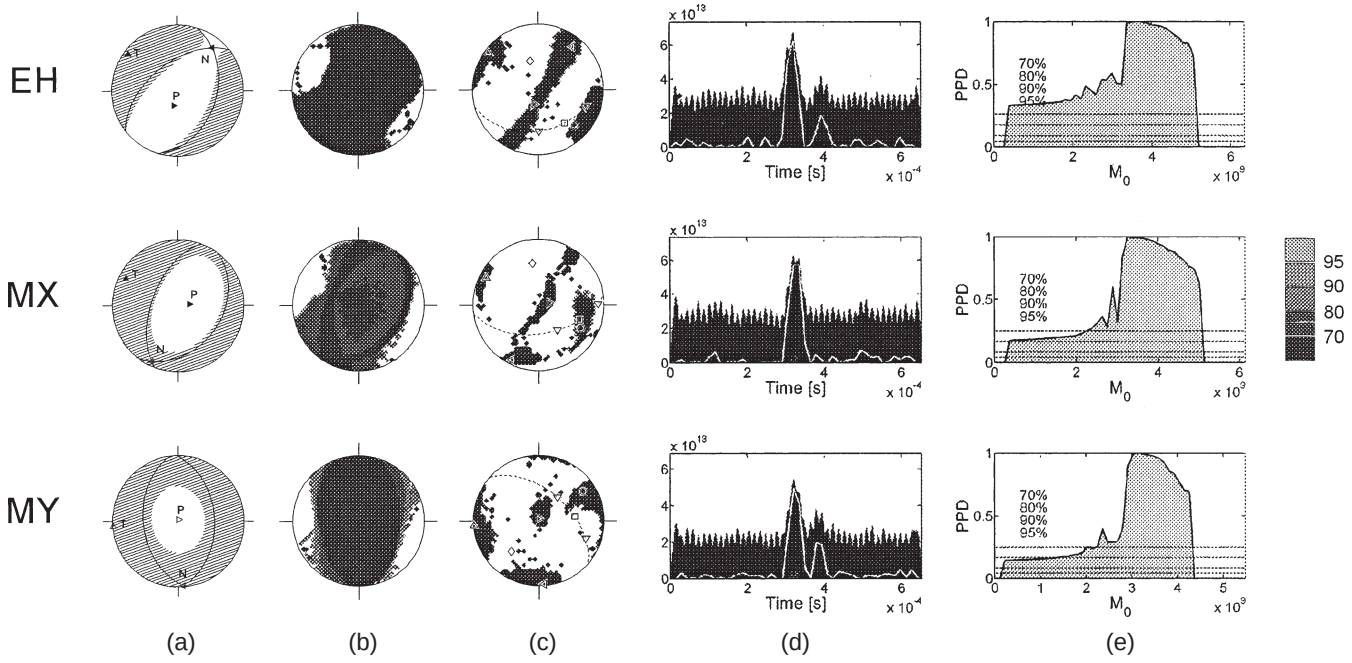

Figure 7. Inversion of noise-free seismograms including the direct and reflected phases by using a simplified Green's function. Five stations considered. For details see the caption of Fig. 4.

are much larger, *cf.* Figs 7 and 4. This success in retrieval of the DC orientation with less than one -third of the stations may seem striking. The reason is obviously in the technique applied to match the synthetics to the observed waveforms. Aiming to accommodate possible differences in arrival times, the synthetics are not compared to the data directly as they are constructed from the Green's function and the current source model, but they are allowed to be shifted within *a priori* defined limits with the criterion of the best correlation to the data. Then, in some stations the synthetics align improperly to the reflected waves instead of the direct ones due to their larger amplitudes, which distorts the mechanism. This is the case, for example of stations 2 (*S* wave at the *z*-component) and 14 (*P* wave at the *z*-component) (see Fig. 8). For other stations, the alignment is correct see, for example, synthetics for station 11 (*S* wave at the components *y* and *z*) in Fig. 8. In the inversion with the five station subset stations 2 and 14 are missing, that is they do not spoil the solution due to their misalignment. Thus, reducing the data set does not necessarily mean obtaining a less accurate solution. The situation just described depends on the configuration of the source, stations and the free surface, and also on the mechanism of the source. Unfortunately, this prevents us selecting *a priori* the stations suitable for the retrieval of the source parameters from real data on the basis of synthetic modelling. Occasional misalignment can hardly be avoided within the automated regime of the inversion. The only way out is to check the final match of synthetics to the data, eliminate the channels where the misalignment occurred, and invert the data set again.

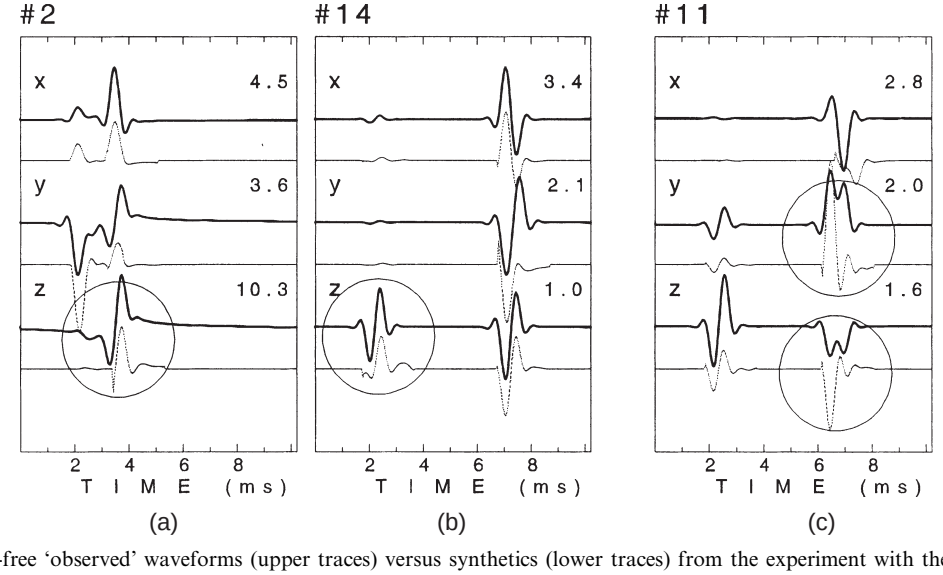

Figure 8. The noise-free 'observed' waveforms (upper traces) versus synthetics (lower traces) from the experiment with the true source location. (a),(b) Inversion for 16 stations (stations #2 and #14 displayed); (c) inversion for only five stations (station #11 displayed).

6 THE URL EVENTS

As an example of application of the above inversion procedure to real experimental data, two events of moment magnitude m_W about -2 observed at the Underground Research Laboratory of AECL, Canada, were analysed. They occurred in the close vicinity of the tunnel face during its excavation and were separated by 4 s. The source of the first event occurred on 1991 September 25, at 16:03:20.400 and was located at the point (0.93, 1.63, 0.76) m, i.e. the point used as a source in synthetic tests described above. The location of the source of the other event (1991 September 25, 16:03:24.790) is 1.68, 0.68, -0.25, that is they are situated only 1.58 m apart. Both events were recorded by the complete URL network (Fig. 1) only station 6 was avoided because of waveform distortion in the signal. The records were filtered with a Butterworth high-pass filter with a cut-off of 100 Hz to eliminate the DC offset; the high-frequency part of the spectrum having a maximum around 6 kHz was not changed by filtering. The records are rather complex and it is not possible to single out the direct and reflected waves from the *P* group and from the *S* group (Fig. 9). Similarly to the synthetic experiments, inversion was performed in two set-ups: including the data from (i)15 stations and (ii) from five stations only (1, 5, 9, 11, 15). The Green's function was constructed for a homogeneous space. The fit of the synthetics, calculated for the inverted mechanism, to the data is rather poor for both the events when the complete data set is processed (results are not shown). At some stations even the major peaks in the records are not well modelled, which suggests that the complete data set may not be fully internally consistent due to unrecognized propagation effects. The fit is slightly better with the reduced data set shown in Fig. 9, in which the results for the later event are displayed. The fit is still rather poor, however, as can be seen on the zoom of the *x*-component of station 1. The mechanism and source time function retrieved for both the event at 16:03:20.400 (I) and the one at 16:03:24.790 (II) using the 15 stations and five stations are shown in Figs 10 and 11, respectively. Even taking into account the uncertainty of about 30° which was recorded in the synthetic experiments as a consequence of neglecting the free surface in the modelling of the medium, the difference in the orientation of the DC part of the source obtained from 16 and five stations is rather high for both the URL events processed. It suggests that the records of individual stations may reflect lateral inhomogeneity of the medium which is not known to us. The only feature which seems to repeat in the results from both the 16 and the five station sets is the pattern of the *T*- and *P*-axes. From this viewpoint, both the events seem to be complementary: the position of the *P*-axis

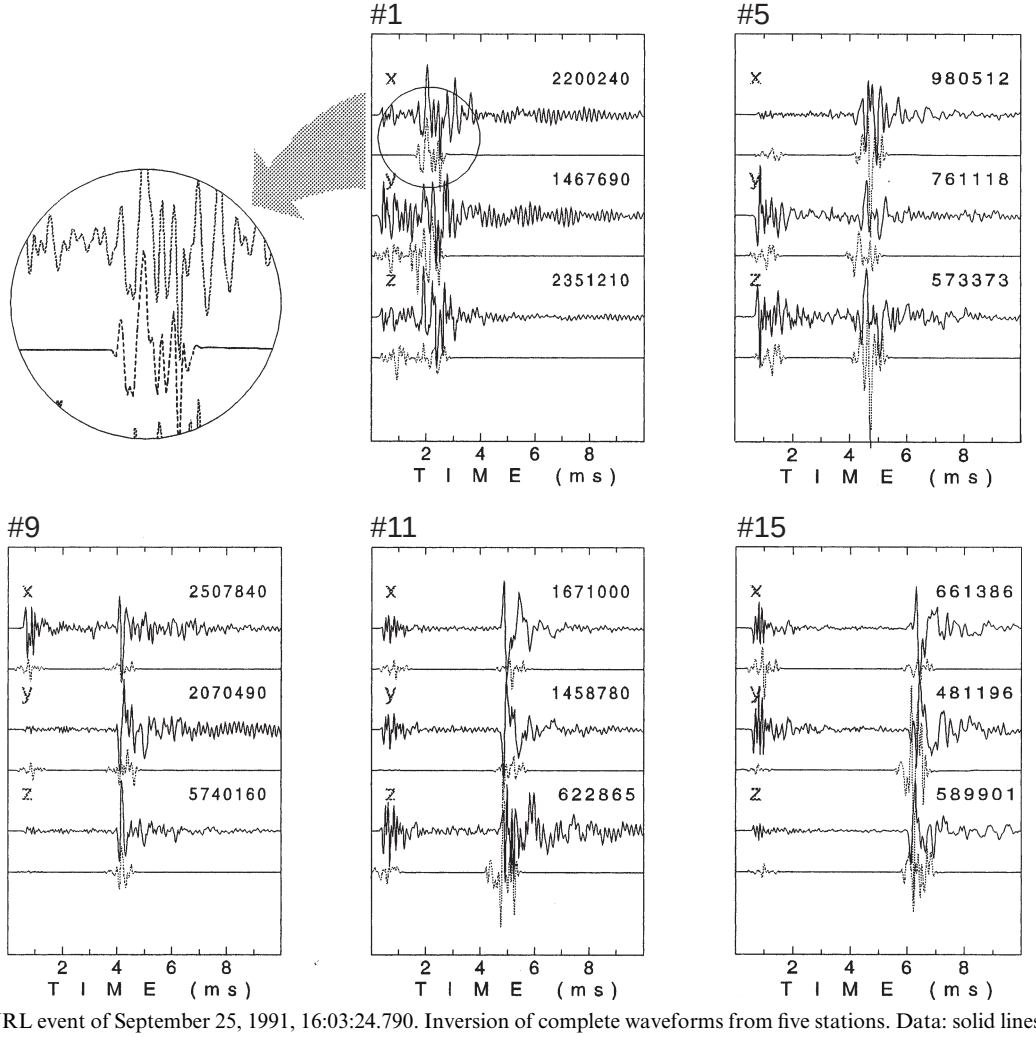

Figure 9. The URL event of September 25, 1991, 16:03:24.790. Inversion of complete waveforms from five stations. Data: solid lines at upper traces; synthetics: dotted lines at lower traces.

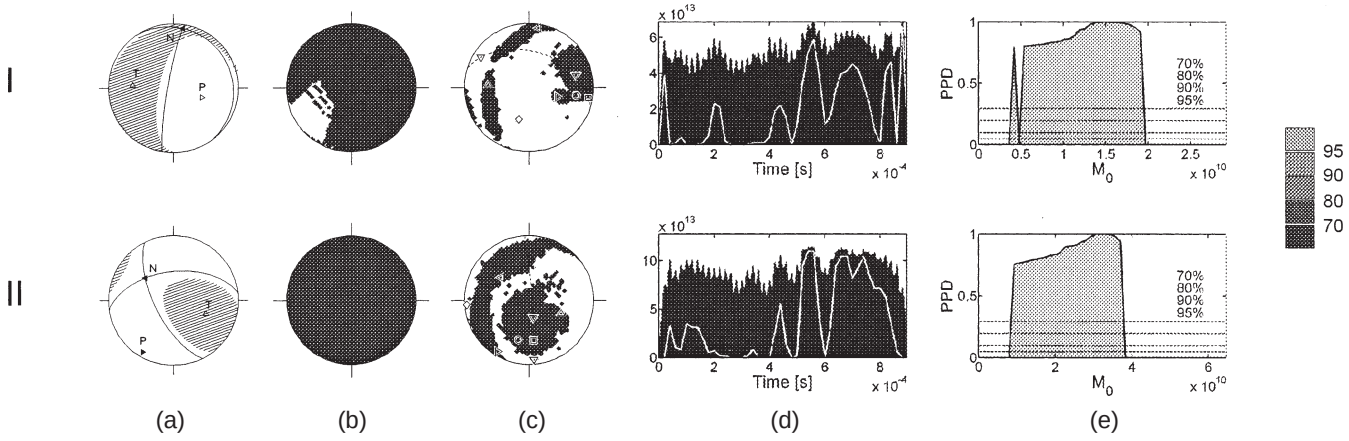

Figure 10. Reconstructed mechanisms and STFs of the URL events (I) of 1991 September 25, 16:03:20.400 and (II) of 1991 September 25, 16:03:24.790; inversion of 15 stations. For explanation of (a-e) see caption of Fig. 4.

of event (I) is roughly replaced by the *T*-axis of event (II). Both mechanisms are largely compensated linear vector dipoles (CLVD) along the *P*-axis (I) and *T*-axis (II). Confidence regions constructed to estimate the error imposed on the retrieved mechanism and STF by neglecting the tunnel face during the Green's function synthesis assigns some weight to this observation: the positions of the *P*-axis for event (I) and of the *T*-axis for event (II) are the most reliably determined parameters of the mechanism, being constrained reasonably at the 70 per cent confidence level. Thus, we may hypothesize that event (I) caused an over-relaxation of the stressed focal zone and the following event (II) partly restored the state of stress.

7 CONCLUSIONS

The inversion algorithm INPAR seems to be fairly robust when applied to data for which a model of the medium is not well constrained. With this algorithm an inconsistency is investigated which originates in our neglecting a reflecting free surface close to the hypocentre during construction of the Green's function. This crude simplification of the Green's function appears to have a small effect when the exact hypocentre is hit. The algorithm provides us with a good estimate of the orientation of the DC and of the source time function. The inconsistency of the model is projected mainly into spurious source components. The gross simplification of the Green's function yields, however, large errors in the formal error analysis. Confidence regions constructed for the *T*-, *N*- and *P*-axes and for the source time function are already wide at the 70 per cent confidence level, which indicates a rather uncertain solution. However, such analysis does not represent much value in practice, because it supposes availability of the exact Green's function, which is not usually the case.

Contamination of the records by a random uniform noise of the level reaching, in turn, 20 and 50 per cent of the peak data amplitude in each channel does not spoil the retrieval of the DC orientation essentially if the hypocentre location is well known. However, the source time function is contaminated largely by spurious signals and error analysis does not help in selecting those related to the source. This stability is surprising taking into account the fact that the 50 per cent noise annihilates the *P* waves in most channels completely, and in some of them masks the direct *S* waves as well. Table 2 summarizes qualitatively results of all experiments.

In studies especially of volcanic seismicity, seismic activity recorded in geothermal areas, and seismicity induced by mining, non-DC components are frequently reported. It was demonstrated that they may be spurious due to non-planar fault surface

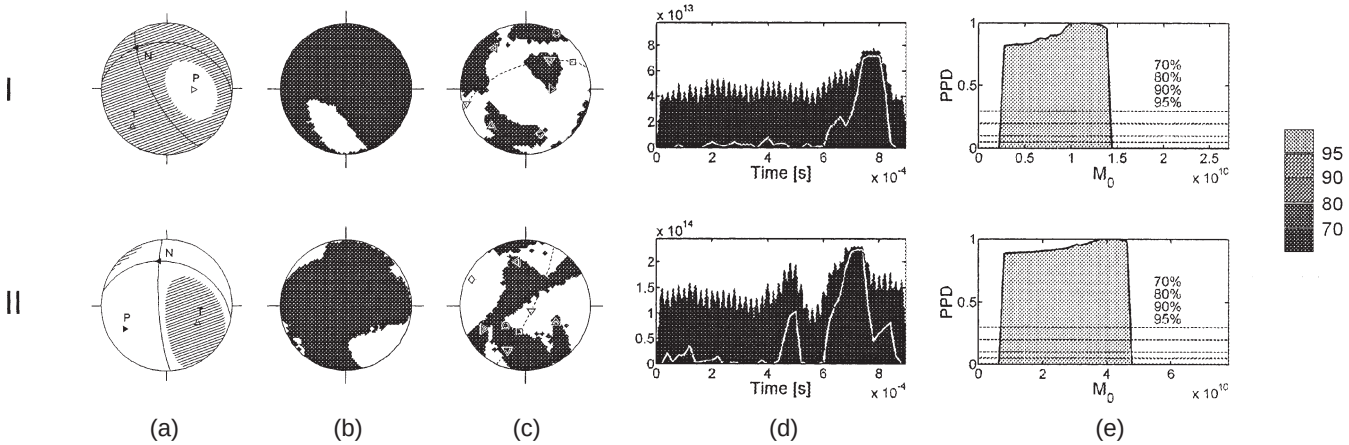

Figure 11 Reconstructed mechanisms and STFs of the URL events (I) of 1991 September 25, 16:03:20.400 and (II) of 1991 September 25, 16:03:24.790; inversion of five stations. For explanation of (a-e) see caption of Fig. 4.

Table 2. A qualitative summary of distortion of the retrieved mechanism as concerns its orientation (Small/Large) and appearance of spurious non-DC components (Yes/No), and distortion of the source time function (Yes/No) in the experiments described in sections 3–5.

Configuration	Noise	Hypocentre	Distortion of mechanism		Distortion of STF
			orientation	non-DC	
16 stations	No	exact	S	Y	N
		mislocated	L	Y	Y
	50%	exact	S	Y	N
		mislocated	L	Y	Y
5 stations	No	exact	S	Y	Y
		mislocated	L	Y	Y
	20%	exact	S	Y	Y
		mislocated	L	Y	Y

(Frohlich 1994), noise contamination (Šílený *et al*. 1996), inexact modelling of the structure and imperfect location of the hypocentre (Kuge & Lay 1994), mismodelling of the inhomogeneity (Kravanja *et al*. 1999) and of anisotropy of the medium (Šílený & Vavryčuk, 2000). We showed here that they may also be an artefact of mismodelling of the interfaces.

ACKNOWLEDGMENTS

This study was partly supported by EC-INCO-Copernicus grant #IC 15 CT96 200, and the Acad. Sci. Czech Rep. Grant Agency grant #A3012904. Part of the study was carried out when J.S. was at the Abdus Salam ICTP at Trieste, Italy, in the framework of the Associated Membership Scheme.

REFERENCES

Campus, P., Suhadolc, P., Panza, G.F. & Šílený, J., 1996. Complete moment tensor retrieval for weak events: application to orogenic and volcanic areas, *Tectonophysics,* **261,** 147–164.

Carlson, S.R. & Young, R.P., 1993. Acoustic emission and ultrasonic velocity study of excavation-induced microcrack damage in the mine-by tunnel wall at the underground research laboratory, Pinawa, Manitoba, *Int. J. Rock Mech. Min. Sci.,* **30,** 901–909.

Červený, V., 2000. *Seismic Ray Theory,* Cambridge University Press, Cambridge, in press.

Falls, S.D. & Young, R.P., 1998. Acoustic emission and ultrasonic-velocity methods used to characterise the excavation disturbance associated with deep tunnels in hard rock, *Tectonophysics,* **289,** 1–15.

Frohlich, C., 1994. Earthquakes with non-double-couple mechanisms, *Science,* **264,** 804–809.

Gajewski, D. & Pšenčík, I., 1990. Vertical seismic profile synthetics by dynamic ray tracing in laterally varying layered anisotropic structures, *J. geophys. Res.,* **95,** 11 301–11 315.

Jílek, P. & Červený, V., 1996. Radiation patterns of point sources situated close to structural interfaces and to the Earth's surface, *Pure appl. Geophys,* **148,** 175–225.

Kravanja, S., Panza, G.F. & Šílený, J., 1999. Robust retrieval of a seismic point-source time function, *Geophys. J. Int.,* **136,** 385–394.

Kuge, K. & Lay, T., 1994. Data-dependent non-double-couple components of shallow earthquake source mechanisms: effects of waveform inversion instability, *Geophys. Res. Lett.,* **21,** 9–12.

Riedesel, M.A. & Jordan, T.H., 1989. Display and assessment of seismic moment tensors, *Bull. Seism. Soc. Am.,* **79,** 85–100.

Šílený, J., 1997. Moment tensor rate functions from waveforms with non-homogeneous variance, *Geophys. J. Int.,* **131,** 767–769.

Šílený, J., 1998. Earthquake source parameters and their confidence regions by a genetic algorithm with a 'memory', *Geophys. J. Int.,* **134,** 228–242.

Šílený, J. & Vavryèuk, V., 2000. Approximate retrieval of the point source in anisotropic media: numerical modelling by indirect parametrization of the source, *Geophys, J, Int.,* **143,** 700–708.

Šílený, J., Panza, G.F. & Campus, P., 1992. Waveform inversion for point source moment tensor retrieval with variable hypocentral depth and structural model, *Geophys. J. Int.,* **109,** 259–274.

Šílený, J., Campus, P. & Panza, G.F., 1996. Seismic moment tensor resolution by waveform inversion of a few local noisy records—I. Synthetic tests, *Geophys. J. Int.,* **126,** 605–619.

Sipkin, S.A., 1982. Estimation of earthquake source parameters by the inversion of waveform data: synthetic waveforms, *Phys. Earth planet. Inter.,* **30,** 242–259.

Tarantola, A., 1987. *Inverse Problem Theory. Methods for Data Fitting and Model Parameter Estimation,* Elsevier, Amsterdam.

Young, R.P. & Collins, D.S., 1993. *The spatial and temporal distribution of AE/MS source locations following the mine-by tunnel excavation of round 17,* Report #RP017AECL, Atomic Energy Canada Ltd, Kingston, Ontario.